

Observability based beacon configuration and positioning for multicopter localization

Naveen Balaji and Sai Sreekar

I. PROBLEM STATEMENT

The UWB based localization has shown various applications in environmental sensing and navigation techniques. In this project, we have investigated the Observability of UWB-based localization from which optimal placement of UWB sensors is derived. The UWB localization method is based on a fixed UWB sender (anchor) fitted on the wall or structure, and moving UWB receiver (tag) on the drone. The Extended Kalman filter fuses the UWB range information and inertial measurements of the drone to localize it in the region without a GPS signal. The UWB anchor position on the structure is crucial as the UWB signal connection is limited to a particular region. In the first part of the project, anchor nodes' positions are obtained by maximizing a measure of the system's observability in the indoor environment. We show an optimal configuration and affordability of UWB based localization in a simple 3D cube space. The real-world experimental data verifies our proposal for the UWB placement problem. In the last part, we extend this idea of UWB placement in structures like bridges for aerial inspection purposes. Other than observability, the UWB range coverage is incorporated together as a constraint to this problem. Our method shows that on the GPS denied part of the bridges, the drone with UWB sensors could navigate effectively.

II. LITERATURE SURVEY

[1] is the baseline paper of our project. In [1], the case of Mars entry navigation using 4 beacons is discussed. The non-linear Observability analysis was carried out using linearized vehicle dynamics and Lie derivatives approximation by Taylor series were presented. For localization improvement, the objective matrix $O^T O$ was maximized using global optimization method, where O is the observability matrix. The optimization was constrained with having a line of sight from a beacon to the entry vehicle. For a given trajectory case, 3 beacons and 4 beacons configurations

were compared showing the effective configuration at the end.

In the second part of the project, we are extending the idea to place sensors in the constrained 3D environment. The paper [2] solves the sensor placement problem by taking beacon range into account. This criteria is important as observability does not check UWB sensor coverage range. The sensor placement problem formulation in the 2D environment is well designed in this paper. We will incorporate this idea, as in big structures a good optimization strategy is needed other than observability conditions.

III. SOLUTION APPROACH

The minimum number of UWB beacons required to localize a multicopter in 3D space will be discussed. The Observability analysis of two, three and four UWB sensors will be carried out. Based on the different positions of UWB anchors, the observability matrix will vary, the optimal configuration (fully observable) can be obtained using this method. The obtained optimal UWB position will be verified by the localization accuracy of the simulation data. The localization accuracy with three and four beacon configuration with real world data will be presented. Once the optimal position with 3 UWB sensors is obtained, the same geometric configuration can be generalized to large environment/structure. The real world experimental data of quadcopter localization with different configuration of UWB anchors will be presented.

In the next section, we investigate about the aerial inspection of industrial structures using the UWB localization. In this project, we considered a generic bridge structure, which needs to be inspected by a drone. The localization constraints will be constructed using the observability and range conditions. The optimal anchor positions on the bridge will be solved using a heuristic optimization method.

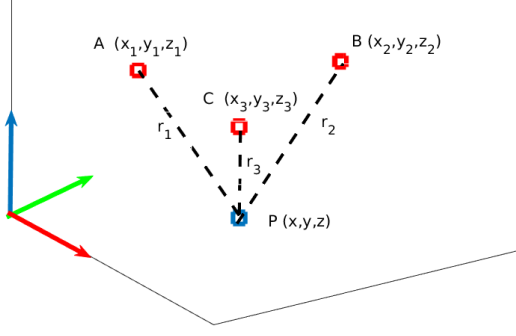


Fig. 1: Point form representation of the system

IV. DYNAMICS OF THE SYSTEM

In this paper, we have chosen the multicopter system for the demonstration purpose. The multicopter system, specifically quadcopter is well studied system in the literature. The quadcopter requires estimation of position (p_x, p_y, p_z) and the orientation (roll, pitch, yaw) for the controlling the vehicle. In this paper, our objective is to estimate the position of the vehicle in inertial frame. The orientation (roll, pitch, yaw) can be estimated by the IMU sensors consistently, and attitude control is implemented at 250 Hz. In this project, we will assume that the attitude system is decoupled and separated from the position controller which runs below 50 Hz.

$$X = [p_x, p_y, p_z, v_x, v_y, v_z]^T \quad U = [a_x, a_y, a_z]^T$$

The states (X) of our system are inertial frame position (x, y, z) and velocity (v_x, v_y, v_z) . The position PID controller produces acceleration in the inertial frame, which will be processed and mapped by the actuator model in the autopilot. The input of our system is the inertial acceleration (a_x, a_y, a_z) . The dynamics of the state transition model is given as

$$\dot{X} = f(X, U) = AX + BU \quad (1)$$

$$A = \begin{pmatrix} 0_{3 \times 3} & I_{3 \times 3} \\ 0_{3 \times 3} & 0_{3 \times 3} \end{pmatrix}, B = \begin{pmatrix} 0_{3 \times 3} \\ I_{3 \times 3} \end{pmatrix}$$

The sensor observational model of system is given as $Y = H(X)$. As we are using multiple sensors the observation model is

$$Y = H(X) = [h_1(X(t)) h_2(X(t)) \dots h_k(X(t))]^T$$

V. LIE DERIVATIVE AND NON-LINEAR OBSERVABILITY

In this section, we present the overview of observability analysis of non-linear systems. Unlike the linear systems, the observability for non-linear system is complicated and determined locally. Lie algebra framework generalizes the concept of geometric controllability and observability for non-linear systems. The Lie derivative is used to obtain the observability matrix. A Lie derivative can be defined as derivative of a scalar along integral curves of vector field. We have considered the quadcopter system described in the previous section.

- 1) The zeroth-order Lie derivative of the sensor measurement function h_k is the same function without any operators.

$$L^0 h_t = h_t$$

- 2) The first-order Lie derivative of function is

$$L^1 h_t = \nabla L^0 h_t \cdot f_t$$

- 3) This trend continues for the i th Lie derivative

$$L^i h_t = \nabla L^{i-1} h_t \cdot f_t$$

where ∇ is the gradient operator, and \cdot is the vector inner product.

Compiling the Lie derivatives, we can get the observability matrix for the non-linear system as

$$\mathcal{O} = \begin{pmatrix} \nabla L^0 h_t \\ \nabla L^1 h_t \\ \dots \\ \nabla L^i h_t \end{pmatrix},$$

The observability matrix should have rank of N for the system to be observable, depending on the system lower order approximation can be made for the observability matrix.

VI. OBSERVABILITY FOR 3 BEACON CONFIGURATION

Figure 1 shows the setup of our system. The three anchor modules of the range sensor (A, B, C) are fixed at the positions (x_i, y_i, z_i) respectively. The UWB tag (receiver) module will be used by the robot to estimate its position. The range data is communicated between the tag and fixed anchor at 10Hz rate. First we have analysed the rigid body position without considering any other system variable into account. For complete position estimation of the tag, the observability matrix

should be of rank three. The range measurement data r_1, r_2, r_3 received by the tag is

$$\begin{aligned} Y_1 = r_1^2 &= (x - x_1)^2 + (y - y_1)^2 + (z - z_1)^2 \\ Y_2 = r_2^2 &= (x - x_2)^2 + (y - y_2)^2 + (z - z_2)^2 \\ Y_3 = r_3^2 &= (x - x_3)^2 + (y - y_3)^2 + (z - z_3)^2 \end{aligned}$$

Considering only the zeroth order Lie derivative approximation of the observability matrix becomes

$$\mathcal{O} = \begin{pmatrix} x - x_1 & y - y_1 & z - z_1 & 0_{3 \times 1} \\ x - x_2 & y - y_2 & z - z_2 & 0_{3 \times 1} \\ x - x_3 & y - y_3 & z - z_3 & 0_{3 \times 1} \end{pmatrix}$$

The rank of the matrix is the dimension of the row space of the matrix. For the matrix to have rank 3 the dimension of row space should be three. The necessary condition is all the three rows have to be linearly independent. It can be seen that each of the rows (upto first three columns) of the \mathcal{O} matrix is the position vector of the UWB tag from the corresponding anchor node.

$$\mathcal{O} = \begin{pmatrix} a_1 \\ a_2 \\ a_3 \end{pmatrix}$$

where $a_i = r - ra_i$ for $i = 1, 2, 3$. The vector r represent position and ra_i represent the anchor position.

- It can be seen that the system is unobservable when the dimension of the row space is less than three (2 or 1).
- Dimension 1 implies that the vectors are collinear.
- Dimension 2 implies that the vectors are co-planar but not collinear.

It can also be observed that for the position vectors to be collinear the anchor nodes themselves have to be collinear and thus Rank-1 can be avoided by not placing the anchor nodes in a straight line.

Rank-2 occurs when the quad-rotor is on the plane formed by the anchor nodes and this is unavoidable as such. However the \mathcal{O} matrix is extended to include the first Lie derivatives along the system dynamics and check the rank of the 6x6 matrix.

In the second part of analysis, we consider our quadcopter system described in eqn 1. The state variables of the system is six (position and velocity). The control input of the system is acceleration vector. We have considered every vector in inertial lab frame. For complete state estimation of the quadcopter, the observability matrix should be of rank six.

The observability matrix of first order approximation (6x6 dimensions) will be

$$\mathcal{O} = \begin{pmatrix} a & 0_{3 \times 3} \\ b & a \end{pmatrix}$$

$$\text{where } a = \begin{pmatrix} a_1 \\ a_2 \\ a_3 \end{pmatrix} \text{ and}$$

$$b = \begin{pmatrix} v_x + a_1 \cdot \frac{\partial v}{\partial x} & v_y + a_1 \cdot \frac{\partial v}{\partial y} & v_z + a_1 \cdot \frac{\partial v}{\partial z} \\ v_x + a_2 \cdot \frac{\partial v}{\partial x} & v_y + a_2 \cdot \frac{\partial v}{\partial y} & v_z + a_2 \cdot \frac{\partial v}{\partial z} \\ v_x + a_3 \cdot \frac{\partial v}{\partial x} & v_y + a_3 \cdot \frac{\partial v}{\partial y} & v_z + a_3 \cdot \frac{\partial v}{\partial z} \end{pmatrix}$$

It can be inferred that when the quadrotor does not lie in the plane formed by the UWBs, the matrix a is of full rank so any combination of the 6 rows can't make the last three columns to zero and hence the rank of observability matrix is 6. Further more when the quadrotor lies in the plane it can be shown that if the velocity vector is not along the plane then the system is observable. To explain and verify the results, we have shown below the cases of collinear and its corresponding rank

A. proof

Let $\lambda_1 a_1 + \lambda_2 a_2 + \lambda_3 a_3 = 0$, where not all λ s are zero. It can be seen that for the linear combination of the 6 rows to be zero the co-efficients to be multiplied with the 4th, 5th, 6th rows are $\lambda_1, \lambda_2, \lambda_3$ respectively.

More over each row of b matrix can be written as

$$\begin{aligned} b_1 &= v^T + a_1 \nabla v \\ b_2 &= v^T + a_2 \nabla v \\ b_3 &= v^T + a_3 \nabla v \end{aligned}$$

Linear combination of b_1, b_2, b_3 provides

$$\lambda_1 b_1 + \lambda_2 b_2 + \lambda_3 b_3 = (\lambda_1 + \lambda_2 + \lambda_3) v^T + (\lambda_1 a_1 + \lambda_2 a_2 + \lambda_3 a_3) \nabla v$$

If $\lambda_1 a_1 + \lambda_2 a_2 + \lambda_3 a_3 = 0$. We get

$$\lambda_1 b_1 + \lambda_2 b_2 + \lambda_3 b_3 = (\lambda_1 + \lambda_2 + \lambda_3) v^T$$

So, if v^T does not belong to the span of a_1, a_2, a_3 then the system is fully observable, even when the quadrotor lies in the plane formed by the beacons.

VII. OBSERVABILITY ANALYSIS FOR 4 ANCHOR NODES

Using the similar approach as above first only the zeroth Lie derivatives are considered giving O as

$$\begin{pmatrix} x-x_1 & y-y_1 & z-z_1 & 0_{3 \times 1} \\ x-x_2 & y-y_2 & z-z_2 & 0_{3 \times 1} \\ x-x_3 & y-y_3 & z-z_3 & 0_{3 \times 1} \\ x-x_4 & y-y_4 & z-z_4 & 0_{3 \times 1} \end{pmatrix}$$

The case with 3 anchor nodes will be used to derive results for the case of 4 anchor nodes.

A. Case-i

If the 4 beacons lie in a plane, then using the similar analysis as before the Rank of the matrix is two when the quad-rotor lies in the plane of the beacons.

B. Case-ii

The beacons are non co-planar, then by taking combinations of 3 beacons together 4 distinct planes are formed.

1) *Proposition:* If P_1, P_2, P_3, P_4 are the four distinct planes formed by taking combinations of 3 beacons together then $P_1 \cap P_2 \cap P_3 \cap P_4 = \phi$

2) *Proof:* Let $p \in P_1 \cap P_2 \cap P_3 \cap P_4$

$p \neq r_1, r_2, r_3, r_4$ as none of the beacons lie on all the 4 planes.

$$p \in P_1 \cap P_2 \cap P_3$$

Without loss of generality consider

$$P_1 = P(r_1, r_2, r_3)$$

$$P_2 = P(r_1, r_2, r_4)$$

$$P_3 = P(r_2, r_3, r_4)$$

$$P_4 = P(r_1, r_3, r_4)$$

$$P_1 \cap P_2 \cap P_3 = (P_1 \cap P_2) \cap (P_2 \cap P_3)$$

As we know that intersection of two planes is a line and let $L(g, h)$ denote the line passing through the points g and h .

Therefore R.H.S of the above equation becomes

$$L(r_1, r_2) \cap L(r_2, r_3)$$

It can be clearly seen that the above two lines intersect at r_2 . But we already know that $p \neq r_1, r_2, r_3, r_4$.

\therefore by proof of contradiction the proposition has been proved.

Therefore the quadrotor can't simultaneously lie on the 4 planes and thus the system is always observable when the 4 beacons are arranged in a non co-planar fashion.

However when the 4 beacons are co-planar using the similar arguments as in the case with 3 beacons it can be shown that the system is still observable when the velocity of the quadrotor is not tangential to the plane formed by the beacons.

VIII. OBSERVABILITY ANALYSIS FOR 2 ANCHOR NODES AND A LIDAR

The output map for the following system will be

$$Y_1 = (x-x_1)^2 + (y-y_1)^2 + (z-z_1)^2$$

$$Y_2 = (x-x_2)^2 + (y-y_2)^2 + (z-z_2)^2$$

$$Y_3 = z^2$$

Considering the zeroth order Lie derivatives the observability matrix will become

$$\begin{pmatrix} x-x_1 & y-y_1 & z-z_1 & 0_{3 \times 1} \\ x-x_2 & y-y_2 & z-z_2 & 0_{3 \times 1} \\ 0 & 0 & z & 0_{3 \times 1} \end{pmatrix}$$

When the first two rows(upto 3 columns), position vectors from quadrotor to the respective beacons are collinear then the rank of the matrix is utmost 2. This happens when the quadrotor lies on the line joining the 2 beacons.

When the quadrotor is not on the line joining the beacons, the two position vectors span a plane. For the rank to be three the third row i.e. $(0, 0, z)$ should not belong to the plane. This means the plane should not be vertical.

The plane is vertical when (x, y) is collinear with (x_1, y_1) and (x_2, y_2) . To see this conduct a thought experiment with the points(projection of the actual points onto the ground) not collinear to observe that the plane formed is oblique.

Also, note that the actual collinearity case mentioned at the starting of the section is a subcase of the projection collinearity condition.

Considering the first order Lie derivatives also we get

$$\begin{pmatrix} a' & 0_{3 \times 3} \\ b' & a' \end{pmatrix}$$

Where a' denotes the above 3×3 matrix and b' denotes

$$b'_1 = v^T + a'_1 \nabla v$$

$$b'_2 = v^T + a'_2 \nabla v$$

$$b'_3 = (0, 0, v_z) + a'_3 \nabla v$$

Using the similar arguments used for the 3 beacon and 4 beacon first order Lie derivative cases we can conclude that even though the projections are collinear when the velocity is not along the line joining the 2 beacons the system is observable.

IX. SIMULATION RESULTS

To verify our theory, we have simulated experiments with three UWB anchor case. Figure 2 shows the two experiment, with their results. We have considered the quadcopter dynamics as described in equation 1.

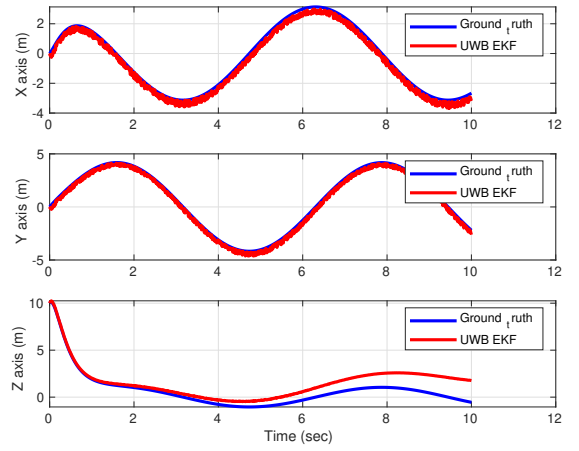
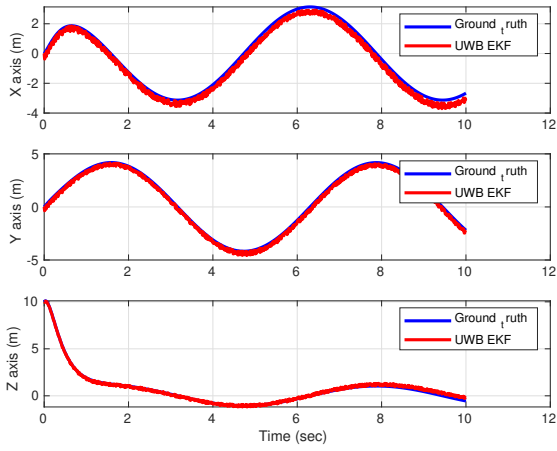
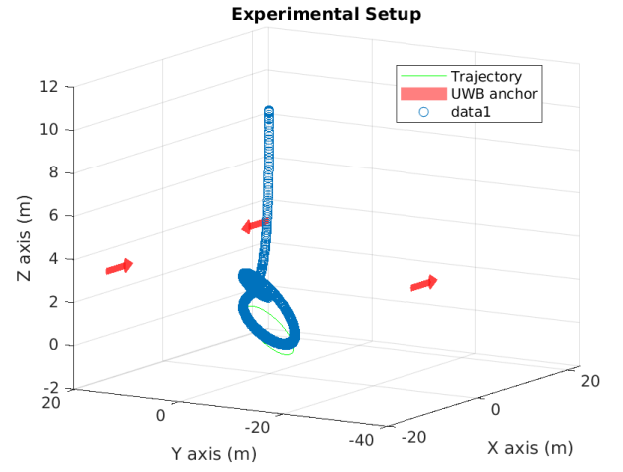
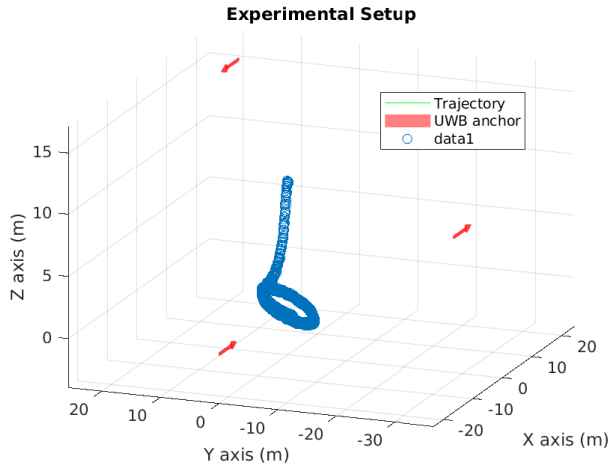


Fig. 2: The two experiments were conducted by varying anchor positions and keeping all other parameters same. The case with anchors located on the same horizontal plane shows inferior results.

The quadcopter was provided with a circular trajectory along horizontal plane and simple movement in vertical plane. The Extended Kalman Filter (EKF) as described in [3] was used to estimate the position of the quadcopter. In the simulation Gaussian noise were incorporated both at the system level and sensor level. In figure 2, the difference between right and left-side experiments is the placement of anchor beacons. In the former case, the anchors are placed such a way that all the three anchors have different (x, y, z) co-ordinates. In the later case, the anchors were placed in the same horizontal plane. All the other parameters like noise, gains are same in both the case.

The position estimation shown in figure 2 observes that when the anchors are in same horizontal plane, the height (z-axis) estimation is poor. The X and Y position

estimation were good, which says that in observability matrix, the row of z-axis alone not contributing to the rank. The detailed error analysis is shown in 3. The height estimation error grows exponentially in the second experiment.

The similar results were experienced in the real world experiment with UWB sensor. In experiment, where the all UWB anchors placed in same horizontal plane were not able to estimate the height properly. Similar verification can be done for four UWB anchors case.

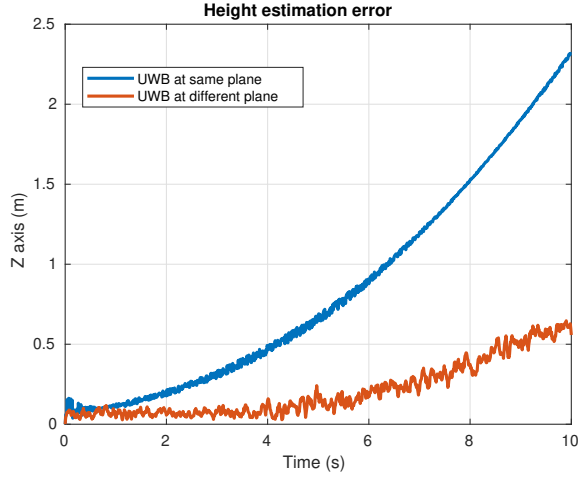


Fig. 3: Error comparison of the two experiments

X. OPTIMAL SENSOR PLACEMENT

The UWB localization method is based on a fixed UWB sender fitted on the wall or structure, and moving UWB receiver on the drone. The UWB sender position on the structure is crucial as the UWB signal connection is limited to a particular region. In this paper, we have experimented with a widely used UWB module in the market to model its range coverage on the 3D space. The results of a single UWB sender and receiver 3D model is used in the sensor placement problem. We have formulated an optimization problem of the UWB sender position using its range model in a constrained industrial environment. The primary constraint is a minimum of three UWB sensors should be in communication with the drone for steady localization. Our objective is to increase the localization region around the industrial structure by placing minimum UWB senders. We have simulated a large jib crane as an industrial structure in the GPS-denied environment to validate our method. This UWB sensor placement problem is of NP-hard type, that is no direct methods are available to find the optimal solution. We present our heuristics method to find the sub-optimal solution to the problem. The same solution can be applied to other industrial structures such as turbine and bridges for reliable aerial inspections.

A. Methodology

For each point in space, the localization constraint of maintaining the connection with three or more UWB anchors has to be satisfied to qualify as signal covered point. The other points in space which cannot satisfy this constraints are termed as uncovered points. The

main objective of the problem is to maximize the covered points in the space by placing the anchors on the crane model.

We considered the 3D space of $30m \times 80m \times 80m$ as a set of discrete grids. The resolution of each grid is 1m. The function made by us, iterate through each grid in the 3D space and stores the neighboring anchors in its connectivity range. The grid cell will then be evaluated for the localization constraint to classify it as a covered point or uncovered point. Depending on the type, it is stored on its respective sets. Note that the approximate area's accuracy depends on the size of grids, we have to iterate on this to achieve reasonable solutions.

For proceeding to compute the coverage area, we have input the UWB anchor positions. The UWB anchor should be placed in the domain of the crane in the 3D space. We have to take the directional nature of the antenna also in account to solve this problem. The proposed approach uses the idea of computational geometry to come up with the solutions. The following steps are followed by us to achieve the solution.

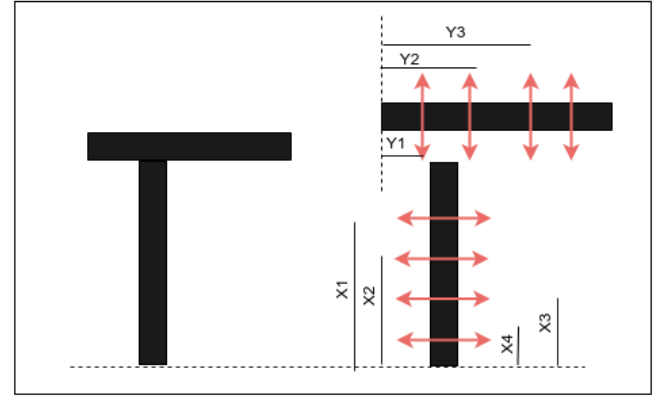


Fig. 4: The crane placement problem is modelled into a dimensional optimisation problem

The each double-side arrow presents the 4 UWB sensors on a square configuration with the inward side. Figure 4 shows the side view of crane, the inward side is of small order and symmetrical. The UWB anchors will be placed symmetrically on the opposite inboard side of the crane. The crane placement problem was further simplified as a 1D, by considering the vertical and horizontal bar as independent set. As the length of both the bars are same order. We considered a set of 5 arrows for each of the bar. Now the sensor optimization problem is simplified in solution search. Our variables in the problem is $[x_1, x_2, x_3, x_4, x_5, y_1, y_2, y_3, y_4, y_5]$. All the variables inequality constraints are linear and inde-

pendent. We can solve the optimization by employing heuristics solver such as Particle Swarm Optimization (PSO) as these solver does not need any gradient evaluations. We can model the optimization problem as

$$S^* = \operatorname{argmax} f(x_1, x_2, x_3, x_4, x_5, y_1, y_2, y_3, y_4, y_5)$$

$$0 < x_i, y_i < 60 \quad i = 1, 2, 3, 4$$

where function (f) denotes the total grid points covered by the complete set of UWB anchors.

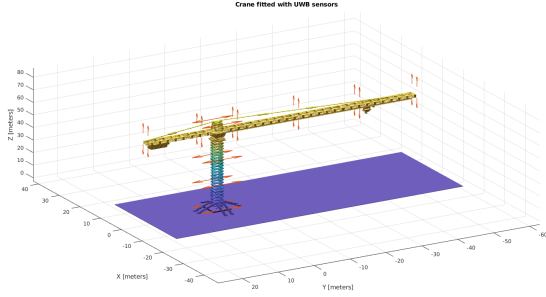


Fig. 5: The placement of UWB anchors on the crane were showed by the red arrow (arrow depicts sensor forward direction)

B. Numerical Results

The above described approach is applied to 3D scenario of the jib-crane in the MATLAB. We have considered the simplistic cuboid case corresponding to the spaces of $30m \times 80m \times 80m$. Figure 5 represents the crane structure, needed to be inspected by drones. The aim is to determine the UWB anchors position such that it maximizes the number of coverage zones in the given space. The placement of UWB anchors at the crane with the proposed method is shown in Fig. 5. The red arrow shows the UWB anchors representing their forward direction placed on the edge of crane.

Figure 6 shows the covered points in the space obtained by the method of UWB placement. The crane with the arrows depicting the UWB anchors can be seen in the image. The blue dots depicts the covered points that satisfied the localization constraints. The covered points by our approach are able to achieve 91.3% coverage. We have used only 40 modules in this experiment to get effective results.

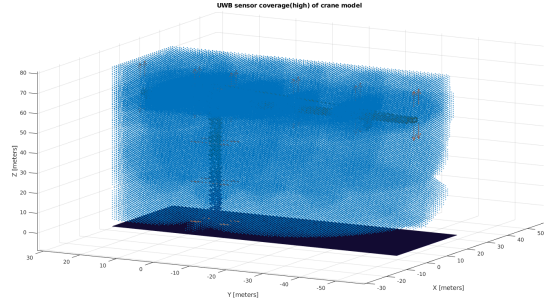


Fig. 6: The blue points shows the sensor coverage points sufficient for localization

XI. OPTIMAL CONTROL FOR GOOD OBSERVABILITY

Seeing that Observability plays a vital role in accurate navigation we formulated an Optimal Control problem to optimize the trajectory of the Quadrotor for good Observability. [4] mentions various ways of bringing in a measure of observability like introducing a determinant inequality constraint on the system, an additional cost term to deal with observability. The method of adding inequality constraint brings in a problem in the form of choosing the choice of threshold, and ensuring that a trajectory indeed exists where the inequality is met. We employ the second method by introducing an additional cost term in the Performance index.

The determinant of the 6x6 Observability matrix is the square of the determinant of the 3x3 Observability matrix. Hence the additional cost term is decided as $1/\det^2(O)$.

The O matrix is modified to $\frac{1}{r_1 r_2 r_3} a$.

$$J = \int_0^{t_f} \left(\frac{1}{\det(O)^2} + \frac{1}{2} (X - X_d)^T (X - X_d) + \frac{1}{2} u^T u \right) dt$$

From Pontryagin's Maximum Principle we have

$$H_u = 0 \implies u = -B^T \lambda$$

$$H_x + \lambda \cdot T = 0$$

$$H_x = \frac{\partial \left(\frac{1}{\det(O)^2} \right)}{\partial X} + (X - X_d)^T + \lambda^T A$$

For the purpose of ease of computation the fixed end time problem has been modelled resulting in the transversality condition $\lambda(T) = 0$

Consider the first term in H_x expression

$$\implies \frac{-2}{\det(O)^3} \frac{\partial \det(O)}{\partial X}$$

$$\frac{\partial \det(O)}{\partial X} = \frac{\partial \left(\frac{1}{r_1 r_2 r_3} \right)}{\partial X} \det(a) + \frac{1}{r_1 r_2 r_3} \frac{\partial \det(a)}{\partial X}$$

$$\text{Writing } \det(a) = -(1 - [x, y, z] P^{-1} [111]^T) \det(P)$$

Where P is the following matrix

$$\begin{pmatrix} x_1 & y_1 & z_1 \\ x_2 & y_2 & z_2 \\ x_3 & y_3 & z_3 \end{pmatrix}$$

$$\Rightarrow \frac{\partial \det(a)}{\partial X} = [111]P^{-1}[I_{3 \times 3} 0_{3 \times 3}] \det(P)$$

Substituting the above expressions in H_x we get

$$\begin{aligned} & \frac{2}{\det(O)^2} (\sum_{i=1}^3 \frac{a_i}{|a_i|^2} 0_{1 \times 3}) \\ & + \frac{-2}{|a_1||a_2||a_3|\det(O)^3} [111](P^T)^{-1}[I_{3 \times 3} 0_{3 \times 3}] \det(P) \\ & - [(x - x_d)^T 0_{1 \times 3}] + \lambda^T A \end{aligned}$$

Thus we have state and Co-state's dynamics equations, with initial condition on state and final condition on costate. The control input has to be chosen in such a way that the boundary conditions on state and costate are satisfied along with $H_u = 0$ at every instant.

Gradient descent method is applied to find the optimal control. The initial choice of control was PD, integrated forward to obtain the states at every instant, using the states the co-states are integrated backwards. Then H_u at every instant is checked and u of every instant is changed to $u(t) - \alpha H_u(t)$ which is then used to integrate state forwards and then co-state backwards. The process is repeated till the error in H_u is less than a threshold.

XII. RESULTS

The formulated Optimal Control problem has been tested with the following considerations.

P is

$$\begin{pmatrix} 10 & 0 & 0 \\ 0 & 15 & 0 \\ 0 & 0 & 10 \end{pmatrix}$$

The initial state of the quadrotor as

$$(8 \ 9 \ 11 \ 0 \ 0 \ 0)$$

The desired position as

$$(14 \ 15 \ 17)$$

The final time was selected using hit and trial as 2.32 s. Below is the graph comparing the trajectories from PD control and the formulated Optimal Control. One apparent drawback of the formulated Optimal Control is that the final velocity is not zero, but some mission requirements may demand a zero final velocity. This can be achieved by solving the fixed final state Optimal Control problem, however inferring from the determinant graph it can be concluded that the trade off in final velocity is paid in more Observability.

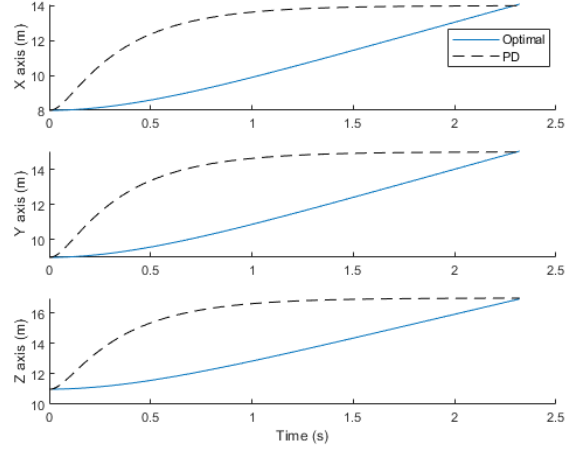


Fig. 7: Trajectory Comparison between PD Control and Optimal Control

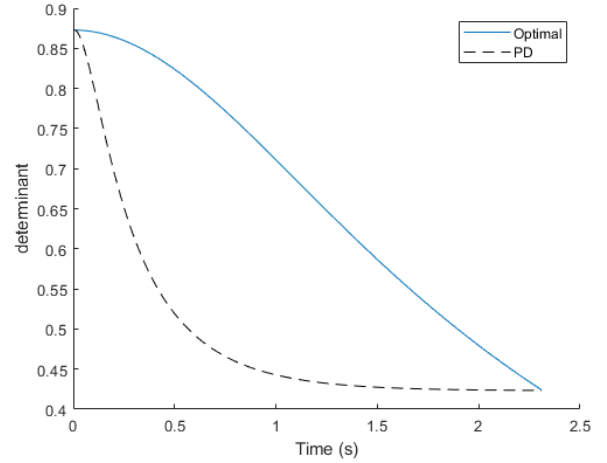


Fig. 8: Observability Comparison between PD control and Optimal Control

XIII. CONCLUSION

In this paper, we have introduced the observability analysis of non-linear systems. We have considered the observability analysis for the quadcopter system localizing with the range based beacon in indoor environment. We provided the observability matrix for the 2 UWB, 3 UWB and 4 UWB anchor case. We verified our theory using the simulation in the 3 UWB anchor case. The placement of UWB anchors plays a vital role in the accuracy of state estimation.

REFERENCES

- [1] Yu, Zhengshi, Pingyuan Cui, and Shengying Zhu. "Observability-based beacon configuration optimization

- for Mars entry navigation." *Journal of Guidance, Control, and Dynamics* 38.4 (2015): 643-650.
- [2] Laguna, M., Roa, J.O., Jiménez, A.R. and Seco, F., 2009. Diversified local search for the optimal layout of beacons in an indoor positioning system. *Iie Transactions*, 41(3), pp.247-259.
 - [3] N. Balaji, M. Kothari and A. Abhishek, "GPS Denied Localization and Magnetometer-Free Yaw Estimation for Multi-rotor UAVs," 2020 International Conference on Unmanned Aircraft Systems (ICUAS), Athens, Greece, 2020, pp. 983-990, doi: 10.1109/ICUAS48674.2020.9213895.
 - [4] Christoph Böhm, Rolf Findeisen, Frank Allgöwer, Avoidance of Poorly Observable Trajectories: A Predictive Control Perspective, *IFAC Proceedings Volumes*, Volume 41, Issue 2, 2008, Pages 1952-1957, ISSN 1474-6670, ISBN 9783902661005, <https://doi.org/10.3182/20080706-5-KR-1001.00332>.